2016

# Characterization and Performance Testing of Two-Stage Reciprocating Compressors during the Dynamic Charging of a Tank with Air

Xinye Zhang
*Purdue Univesity, United States of America*, zhan1600@purdue.edu

Bin Yang
*Purdue Univesity, United States of America*, yang62@purdue.edu

Andres Osorio
*BlackPak Inc*, aosorio@blackpaktech.com

Dylan Bethel
*BlackPak Inc*, dbethel@blackpaktech.com

Orkan Kurtulus
*Purdue Univesity, United States of America*, orkan@purdue.edu

***See next page for additional authors***

**Authors**
Xinye Zhang, Bin Yang, Andres Osorio, Dylan Bethel, Orkan Kurtulus, and Eckhard Groll

# Characterization and Performance Testing of Two-Stage Reciprocating Compressors during the Dynamic Charging of a Tank with Air

Xinye Zhang[1*], Bin Yang[1], Orkan Kurtulus[1], Eckhard A. Groll[1], Andres Osorio[2], Dylan Bethel[2]

[1] Purdue University, Ray W. Herrick Laboratories, West Lafayette, IN, USA
xinye@purdue.edu, yang62@purdue.edu, orkan@purdue.edu, groll@purdue.edu

[2] BlackPak Inc. San Leandro, CA, USA
aosorio@blackpaktech.com, dbethel@blackpaktech.com

* Corresponding Author

## ABSTRACT

Relatively little information is available in the literature with respect to performance of compressors used during the dynamic charging process of a tank. Therefore, work presented in this paper focuses on experimental performance testing of a two-stage reciprocating compressor system using air as the working fluid during the dynamic charging of a tank. A new open loop system test stand, has been designed and built to conduct the dynamic compressor performance tests. Testing was conducted from an initial pressure of 101.3 kPa to a final tank pressure of 3600 kPa. To achieve the final pressure of 3600 kPa, two hermetic reciprocating compressors were used in series. Due to the nature of the charging process, initially only the first stage compressor was activated until the tank pressure reached a level that required activation of the second stage compressor.

Along with the experimental effort, a simulation model to predict compressor dynamic performance has been developed. In this model, the initial clearance factors of the two compressors were calculated based on available compressor maps. The calculated clearance factors were then used as inputs to the dynamic model. The entire charging process was then simulated to provide the compressor performance data as a function of time. Finally, the predicted performance was validated using the acquired test data also presented in this paper.

## 1. INTRODUCTION

Various methods have been proposed to model the dynamic process of the reciprocating compressor using air as the working fluid. Elhaj et al. (2008) developed a two-stage reciprocating compressor model performing under various conditions for the development of diagnostic features for predictive condition monitoring. Ndiaye and Bernier (2010) presented a dynamic model of a hermetic reciprocating compressor in on–off cycling operation that accounts for the important phenomena influencing the suction and discharge mass flow rates and the electrical power drawn by the compressor using readily available data from manufacturers. MacLaren and Kerr (1969) created a model that could be applied to a two cylinder high speed refrigeration compressor that accounted for unsteady flow pressure prediction in the valve chamber (for capacity and energy consumption considerations), and at the manifold end (for muffling effectiveness consideration). The model developed by MacLaren and Kerr (1969) had experimental data validation but focused on the discharging process only.

However, little work has been found in open literature relative to experimental validation of the dynamic charging process and charging times. Also, there is little information about how to find the intermediate pressure when the 2*nd* stage compressor begins contribution to the dynamic process. The purpose of this paper is to fill this gap in the open literature using experimental data to find the maximum attainable pressure and temperature of the compressor system and acquire charging times for different target pressures. Furthermore, a simulation model has been formulated to predict the charging process. Experimental data are needed to validate the model predictions.

## 2. EXPERIMENTAL RESULTS

### 2.1 Description of system and experiments

The schematic of an open loop system test stand is shown in Figure 1. The test stand is designed to withstand pressures of up to 14 MPa (140 bars) by using stainless steel piping. A silencer and strainer, filled with desiccant, is used at the inlet of the open loop and installed before the compressor box to avoid moisture and dust contamination of the air. One manual ball valve is located after the dryer to shut off the air flowing into the compressor box, if necessary. After the compressor box, a sight glass is used to check for oil in the compressed air stream. A check valve is also used to prevent any air backflow from the pressurized tank. Furthermore, a mass flow meter is installed to measure the mass flow rate of air after the compressor box. A pressure gauge with a 0 – 7 MPa pressure range indicates the high side pressure directly to the operator for control and safety purposes. Also, a pressure relief valve with a 6 MPa cracking pressure is used to protect the tank from uncontrolled pressure increases. At the end of the open loop, a compressed natural gas (CNG) tank with a service pressure ceiling of 25 MPa is used for storage of the compressed air. A power meter was installed to measure the electric power input and all measured data is obtained and displayed using a DAQ-PC system.

One compressor box is connected to the test stand that leverages two hermetic reciprocating compressors in series to achieve the system target pressure in the storage tank. An electronic box is installed inside the compressor box, which contains an ON/OFF switch, status indicator lights, and a remote control button. Two adjustable pressure switches are located downstream of the first-stage compressor and in the discharge line of the compressor box. The first pressure switch is used to control the activation of the second-stage compressor. Once the system reaches a predefined set pressure, the second compressor begins contributing to the system pressure rise. The second pressure switch is used for safety purposes to shut down the whole system after reaching a predetermined discharge pressure. Two intercoolers, located after each compressor, are used to cool down the discharge gas temperatures. Two oil separators and filters were also used after each compressor to provide access to conduct the oil measurements.

### 2.2 Test stand instrumentation

All measuring instrumentation is indicated in the schematics shown in Figure 1 . All temperatures were measured with T-type thermocouples with ±0.25 ºC accuracy. The inlet pressure of the open loop test stand was measured with an absolute pressure sensor that has an advertised accuracy of ±0.25%. Other pressures are measured with a gauge pressure sensor that has an accuracy of ±0.13% of full scale. A Coriolis-effect mass flow meter with an advertised accuracy of ±0.1% was installed in the open loop test stand to measure mass flow rates of the gas. Electrical power consumptions of the compressors and the cooling fans were measured with power meters with an accuracy of ±0.04%. A data acquisition system was used to convert the incoming voltages from the measuring instrumentation to digital signals for transfer to a personal computer. The computer uses a proper data reduction program for further data analysis..

### 2.3 Test matrix

A test matrix outlining the operating conditions for the open loop system, is shown in Table 1. The maximum attainable pressure inside the discharge tank was obtained using air as the working fluid. Each test was conducted twice; to ensure the results were repeatable. Tests were conducted using a bisection method with a target pressure resolution of less than 170 kPa. Once the maximum attainable pressure was found, two tests at $P_{max}$+170 kPa and five additional tank charging tests at $P_{max}$ were conducted.

### 2.4 Experimental results

During the tests, the following compressor measurements were recorded: compressor mass flow rate, suction and discharge temperatures, suction and discharge pressures, intermediate pressure and temperature, and compressor power consumption. Using these measurements, the compressor performance was evaluated.

A dynamic test with a 2800 kPa target pressure was conducted first as a shakedown test. Figure 2 shows the variation of air pressures as a function of time. It can be noticed that the intermediate pressure, measured as $P_{42}$ and $P_{43}$, increases significantly when only the $1^{st}$ stage compressor is in operation. This increment rate became smaller once the $2^{nd}$ compressor began to contribute to the system pressure rise. The discharge pressure of the compressor box, increases significantly until reaching the target pressure. Additionally, pressure drop between the discharge pressure and the tank pressures due to the filters, the Coriolis-effect mass flow meter, and the pipe connections can be seen in Figure 2. Once the desired pressure of 2800 kPa is reached, the slope of the decrease in discharge pressure and tank pressure is slightly different. This difference is due to backflow, resulting from unavoidable leakage in the compressors, which leads to a small reduction of the $2^{nd}$ stage discharge pressure. However, once the discharge valve is open, these two pressures decreased at the same slope. Also, it is found that the final $2^{nd}$ stage discharge pressure taken immediately after shut-down is larger than the tank pressure at ambient temperature. The higher discharge pressure is due to the compressors' in-head temperature environment being higher than the holding tank temperature.

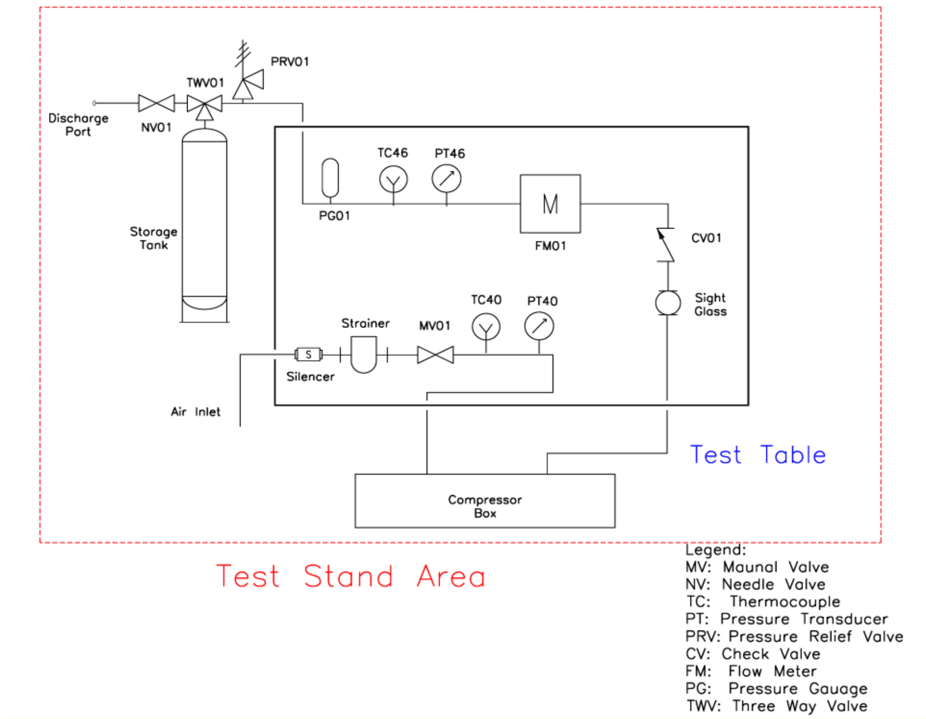


**Figure 1:** Schematic of the open loop system

**Table 1:** Test matrix of dynamic testing with open loop test stand

| Test Number | Target Pressure (kPa) | Failure | Comments |
|---|---|---|---|
| 1 | 2100 | N | Initial low boundary |
| 2 | 4900 | Y | Initial high boundary |
| 3 | 3500 | N | Average of test 1 and 2 |
| 4 | 4200 | N | Average of test 2 and 3 |
| 5 | 4550 | Y | Average of test 2 and 4 |
| 6 | 4375 | N | Average of test 4 and 5. Temporary $P_{max}$ found. |
| 7 | 4550 | Y | $1^{st}$ repetition at $P_{max}$+25 |
| 8 | 4550 | Y | $2^{nd}$ repetition at $P_{max}$+25 |
| 9 | 4375 | N | $1^{st}$ repetition at $P_{max}$ |
| 10 | 4375 | N | $2^{nd}$ repetition at $P_{max}$ |
| 11 | 4375 | N | $3^{rd}$ repetition at $P_{max}$ |

Figure 3 shows the variation of the measured compressed air temperature as a function of time during the open loop testing. Total run time was 30 minutes, which included 3 minutes for warm-up testing, 25 minutes for dynamic testing, and 15 minutes for shut-down testing. During the warm-up stage, only the cooling fans were set to operate. During the shut-down stage, both compressors were shut down at the same time and the discharge valve (NV01) was opened to gradually release the compressed air from tank. In addition, the cooling fans were set to operate until the maximum temperature ($2^{nd}$ stage discharge temperature) dropped to approximately 35 °C.

After the compressor system started, it was found that the $1^{st}$ stage discharge temperature, measured as $T_{41}$, increased significantly once the $1^{st}$ stage compressor started working. Once the $2^{nd}$ stage compressor started working, the discharge temperature of the second compressor increased significantly until it reaches to a final temperature of 75 °C. Another interesting conclusion that can be drawn from Figure 3 is the $1^{st}$ stage discharge temperature was larger than the $2^{nd}$ stage discharge temperature until the run time reached approximately 15 minutes. At that point, the $2^{nd}$ stage discharge temperature climbed dramatically in Figure 3. It can be noticed that the temperature variations after the heat exchanger in both stages were relatively small, which were close to the ambient temperature during the testing. In addition, a small jump of the $2^{nd}$ stage discharge temperature can be seen in the right corner of Figure 3. This small temperature jump is due to the cooling fans being shut off with heat remaining in the compressor system after shut-down.

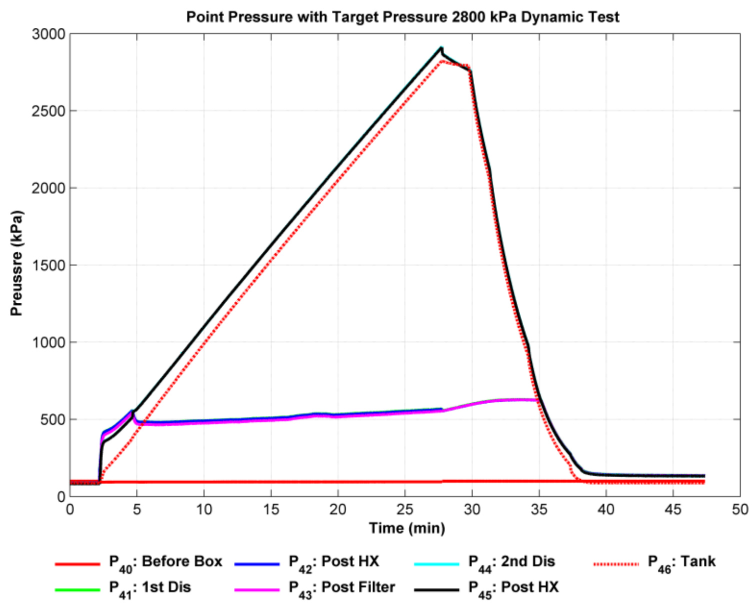


**Figure 2:** Point pressure with target pressure 2800 kPa dynamic test

Figure 4 shows the variation of the pressure ratio, i.e. the ratio of discharge pressure over suction pressure for each stage as a function of time for the tested system. It can be noticed that the pressure ratio of the $1^{st}$ stage compressor is reached immediately once the 1st stage compressor starts operating. This pressure ratio is relatively stable at approximately 5. However, the pressure ratio of the $2^{nd}$ stage compressor increased gradually until the system was turned off. The $2^{nd}$ stage pressure ratio was smaller than the $1^{st}$ stage pressure ratio. Also, it can be seen that the backflow previously discussed has great effects on both pressure ratios by enhancing the intermediate pressures. With increasing intermediate pressure, the $1^{st}$ stage pressure ratio is shown to increase accordingly until the $2^{nd}$ stage pressure ratio drops to approximately 1, which means there is no obvious pressure difference between the inlet and the outlet of the $2^{nd}$ stage compressor. As discussed before, the compressors will hold some pressures at the end of the test, which is the reason why the $1^{st}$ stage pressure ratio is shown to be larger than 1.

To find the maximum attainable pressure inside the discharge tank, several tests were conducted as shown in the test matrix on Table 1. Two selected informative tests will be discussed in this section.

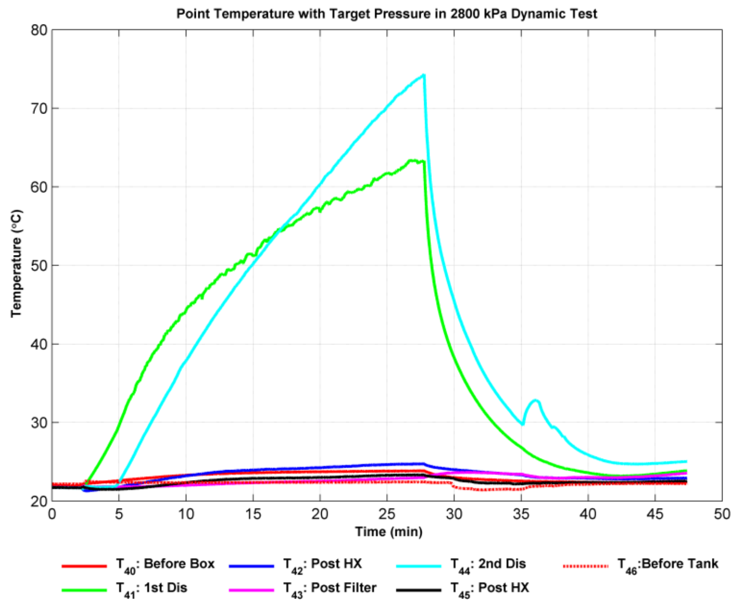


**Figure 3:** Point temperature with target pressure 2800 kPa dynamic test

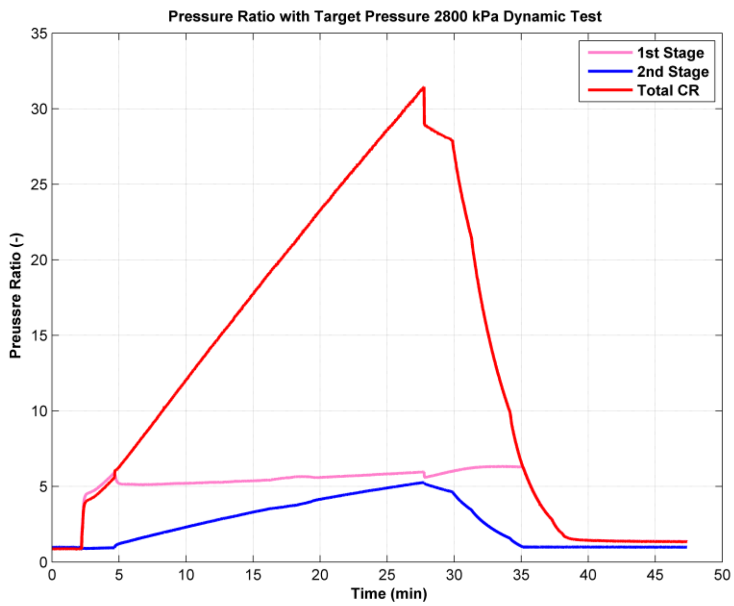


**Figure 4:** Pressure ratio with target pressure 2800 kPa dynamic test

Figure 5 shows the variation of the air pressures as a function of time with a target pressure of 4550 kPa which was set by the pressure switch in the compressor box. It can be noticed that the tank pressure, measured as $P_{46}$, only reached a pressure of 4375 kPa, which is lower than the target pressure. Compared to results in 4200 kPa case, the maximum attainable temperature obtained in the 2$^{nd}$ stage reached a value of 95 °C, which was slightly higher than the maximum temperature during the 4200 kPa test. The reason why the target pressure of 4550 kPa, was not reached is due to the thermal protection installed in the compressor box, which protects the compressor from burning out. Once the low-side operating temperature is higher than the pre-set critical value, the system will automatically shut down due to the thermal protector's engineered design.

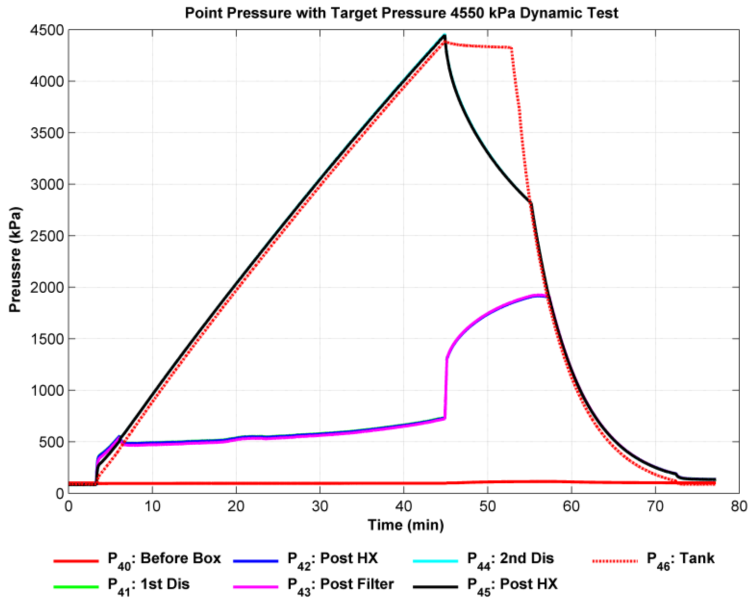


**Figure 5:** Point pressure with target pressure 4550 kPa dynamic test

Based on the discussion above, 4375 kPa is subsequently referred to as the maximum attainable pressure for the system tested. The charging time for this target pressure was 42 min and the maximum discharge temperature was found to be 93 °C at the end of the tests. It can be concluded that the temperature needs to be monitored during the test to ensure the system doesn't shut down due to thermal overloading of the thermal protector.

## 2.5 Oil management

An oil management analysis was conducted during each test. And the differences of the oil weight in the discharge filters during each test were recorded, to gain a general understanding of how oil migrated within the system during testing, as well as general factors that affect oil slippage. This analysis also helped to indicate how much oil was discharged with the compressed air and if additional oil was needed. Three filters were installed after each compression stage. Oil weight data of the various tests performed are shown in Table 2.

It can be noticed that the majority of the oil was discharged by the 1st stage compressor. Also, as expected, more oil was collected during the tests with higher target pressures and longer running time. With that information in-hand, the conclusion can be drawn that the compressors must be recharged with oil after a certain run time, or an oil separator with an automatic oil return must be installed in the system to avoid compressor failure. Furthermore, it should be noted that most of the oil was collected by the first filter which is not shown in Table 2.

**Table 1:** Test matrix of dynamic testing with open loop test stand

| 1st Stage (g) | 2nd Stage (g) | Total (g) | Target Pressure (kPa) | Running Time (min) |
|---|---|---|---|---|
| 3.2 | 0.1 | 3.3 | 2100 | 19 |
| 5.1 | 0.3 | 5.4 | 2800 | 25 |
| 9.9 | 0.2 | 10.1 | 3500 | 30 |
| 12.1 | 0.6 | 12.7 | 4340 | 39 |

Figure 6 shows the variation of the oil slippage as a function of pressure ratio for the 1*st* and 2*nd* stage compressors. It can be seen that the oil slippage of the 1*st* stage compressor increases significantly with higher pressure ratio. This relation can be estimated as a linear curve with an R value of 0.98, as shown in Equation (1). This equation is used to predict oil slippage in the 1st stage compressor. Oil slippage of the 2*nd* stage compressor shows only a minor increase as a function of pressure ratio. The 2nd stage compressor appears to be relatively stable when compared with oil slippage of the 1*st* stage compressor.

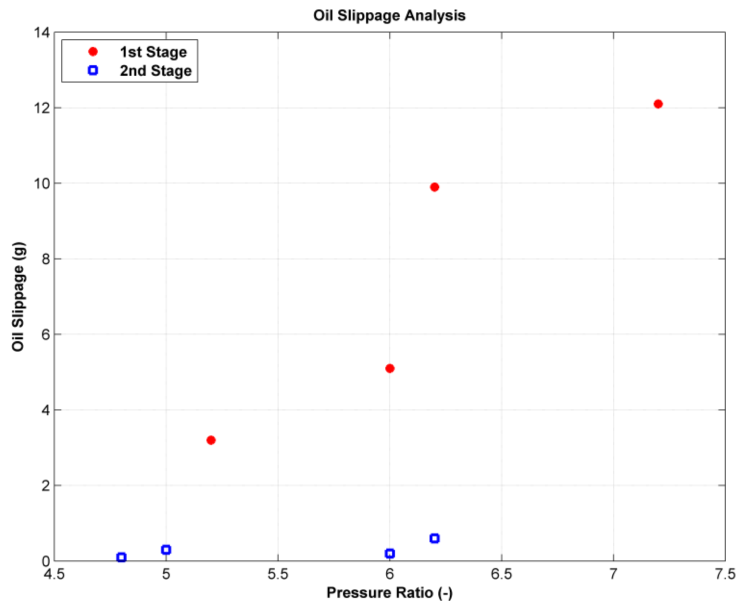


**Figure 6:** Oil slippage with different pressure ratio

$$oil\_slippage = 3.75 \times PR - 0.97 \quad (1)$$

where PR is referred to pressure ratio which should be larger than 1.

Based on the testing performed, it can be concluded that more oil is collected during tests in a two-stage compressor system with higher target pressure. However, if the same target pressures are compared, more oil will be discharged in the lower pressure range by the 1st stage compressor and a smaller amount of oil will be discharged in the 2*nd* stage compressor. In the lower pressure range, high pressure ratios will lead to more significant oil slippage.

## 3. SIMULATION MODEL

A simulation model to predict the compressor dynamic performance has been developed. In this model, the initial clearance factor for the compressor was calculated based on available compressor maps used as an input to the dynamic model. The entire compression process has been simulated to provide compressor performance data as a function of time. Predicted performance will be validated using test data.

### 3.1 Clearance volume factor

The clearance volume factor is a significant value, which affects the performance of compressors. It must be noted that the clearance volume factor is an attribute of the compressor itself and can be found based on experimental results. The approach used here was to find an estimated value based on published compressor performance maps for use in the simulation model.

Compressor map data given by the compressor manufacturer provides the relation between mass flow rate, suction, and discharge conditions. Equation (2) is used to calculate the clearance volume factor. The clearance volume factor C is the slope of the function curve between the volumetric efficiency and the pressure ratio.

$$\eta_v = 1 - C\left[\left(\frac{P_d}{P_s}\right)^{1/m} - 1\right] = \frac{\dot{m}_e}{\dot{m}_{th}} \tag{2}$$

**3.2 Critical intermediate pressure**

Due to the nature of the charging process, the intermediate pressure is not achieved immediately. Initially, only the 1st stage compressor is activated until the tank pressure reaches a level that requires the activation of the 2nd stage compressor. At the beginning of the process, the system pressure is equal to the atmospheric pressure. In two stage compressor systems, the suction volume of the 1st stage compressor is inherently larger than that of the 2nd stage compressor due to the nature of the system design. For the system presented in this work, the discharge gas of the 1st stage compressor flows through the 2nd stage compressor without additional compression occurring and arrives at the storage tank when only the 1st stage compressor runs. The storage tank is used as a back pressure of system. As a response to the gradually increasing back pressure produced by the storage tank, the pressure inside the compressor system as well as the intermediate pressure will increase. In addition, the increasing intermediate pressure will decrease the discharge gas volume. Once the discharge gas volume of the 1st stage compressor is equal to the displacement of 2nd stage compressor, the 2nd stage compressor starts to operate. After this critical condition is achieved, both compressors work in series to compress the gas until the target pressure in storage tank is reached.

Equations (3) to (5) are used to find the critical intermediate pressure value. Since there is no condensation in this system, $\lambda_{\varphi 1} = \lambda_{\varphi 2} = 1$. Due to initial system conditions being set for no compression to occur in the 2*nd* stage compressor, $\varepsilon_2 = 1$, $\eta_{v2} = 1$, $\lambda_{T2} = 1$ in Equation (3).

$$\frac{P_2}{\eta_{v1}} = \frac{V_{h1}}{V_{h2}} \frac{\lambda_{P1}}{\lambda_{P2}} \frac{\lambda_{l1}}{\lambda_{l2}} \frac{\lambda_{T1}}{\lambda_{T2}} \frac{\lambda_{\varphi 1}}{\lambda_{\varphi 2}} \frac{T_2}{T_1} \frac{P_1}{\eta_{v2}} \tag{3}$$

$$\eta_v = 1 - C[(\frac{P_2}{P_1})^{1/m} - 1] \tag{4}$$

by Combining equation (3) and (4), the simplified Equation (5) can be obtained as follows:

$$\frac{P_2}{1 - C\left[\left(\frac{P_2}{P_1}\right)^{1/m} - 1\right]} = \frac{V_{h1}}{V_{h2}} \frac{\lambda_{P1}}{\lambda_{P2}} \frac{\lambda_{l1}}{\lambda_{l2}} \frac{T_2}{T_1} P_1 \lambda_{T1} \tag{5}$$

Parametric data for these equations can be found in the compressor data sheet, and the clearance volume factor can be obtained from Section 3.1. In addition, it can be assumed that $\lambda_{P1} = 0.97$, $\lambda_{P2} = 0.98$, $\lambda_{l1} = \lambda_{l2}$, *and* $\lambda_{T1} = 0.97$. Armed with those assumptions, the critical intermediate pressure has been calculated to be 490 kPa for the given system.

**3.3 Dynamic charging process**

In two-stage compressor systems, the intermediate pressure observes the principle that the discharging gas volume from the 1st compressor will be completely transferred to the 2*nd* stage compressor. However, the corresponding intermediate pressure depends on the relationship between the two compressor displacements. It should be noted that when the discharge condition of the 1*st* stage compressor changes, the gas volume of 2*nd* compressor and the intermediate pressure will respond accordingly. Therefore, the intermediate pressure needs to be adjusted in the simulation to satisfy both compressor displacements. The intermediate pressure between any two stages in a multi-stage compressor system can be calculated using Equation (6) :

$$V_{hj} \frac{\eta_{vj} \lambda_{Tj} \lambda_{Pj} \lambda_{lj}}{\lambda_{\varphi j}} \frac{P_j}{P_1} \frac{T_1}{T_j} = V_{hj+1} \frac{\eta_{v,j+1} \lambda_{T,j+1} \lambda_{P,j+1} \lambda_{l,j+1}}{\lambda_{\varphi,j+1}} \frac{P_{j+1}}{P_1} \frac{T_1}{T_{j+1}} \tag{6}$$

where $j$ is referred to the 1*st* stage and $j + 1$ is referred to 2*nd* stage in a two-stage system

Once the intermediate pressure is found, Equations (7) to (9) can be used to simulate the dynamic compression process and predict all parameters for every time step until the target pressure is achieved. The volumetric efficiency ($\eta_v$) can be obtained from Equation (4).

$$\dot{m}_{dis} = \eta_v V_h \rho n / 60 \tag{7}$$

$$m'_{\text{tank}} = m_{\text{tank}} + \dot{m}_{dis} t_{step} \tag{8}$$

where $t_{step}$ is the time step in each loop.

$$P_{\text{tank}} = \frac{m_{\text{tank}} R_g T_{\text{tank}}}{V_{\text{tank}}} \tag{9}$$

It must be noted that the tank temperature, $T_{tank}$, which is a key parameter used for calculation of the tank pressure is still unknown in Equation (9). Therefore, the storage tank is modeled as a lumped system within the simulation model to calculate the temperature during the charging process as shown in Equations (10) and (11).

$$Q_{loss} = (T_{\text{tank}} - T_{sur}) \times \rho_{air} \times C_{p,air} \times V_{\text{tank}} \left[ 1 - \exp\left( \frac{-hA}{C_{p,air} V_{\text{tank}}} t \right) \right] \tag{10}$$

where $T_{sur}$ is the surrounding temperature of the storage tank.

$$m'_{\text{tank}} u'_{\text{tank}} - m_{\text{tank}} u_{\text{tank}} = m_{\text{tank}} Q_{loss} + \dot{m}_{dis} t_{step} h_L \tag{11}$$

where $h_L$ is the air entering enthalpy to tank and $u_{\text{tank}} = f(T_{\text{tank}})$

Figure 7 shows the variations of pressure with time as predicted by the simulation model. When the target pressure is 2800 kPa, the total charging time is predicted to be approximately 20 minutes, which is validated by the experimental data as discussed above. It is noticed that the 2$^{nd}$ stage compressor does not work until the intermediate pressure reaches 525 kPa, which satisfies mass flow rate matching between the two compressors. In addition, the maximum pressure ratios were 7.2 and 3.91 of the 1$^{st}$ stage and 2$^{nd}$ stage compressors, respectively.

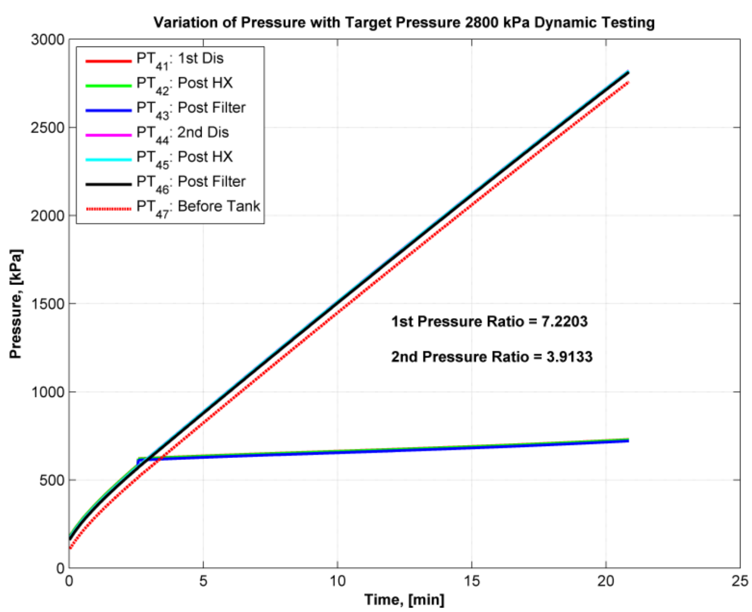


**Figure 7:** Variation of pressure with target pressure 2800 kPa charging process

## 4. CONCLUSION AND FUTURE WORK

This paper presents the experimental performance testing of a two-stage reciprocating compressor systems using air as the working fluid during the dynamic charging of a tank. In addition, a simulation model to predict the compressor performance is discussed as well. The following conclusions can be drawn.

- Several results with different target pressures and run times have been conducted. The following parameters have been recorded: pressures, temperature, surface temperatures, and pressure ratios. In addition, the maximum attainable pressure and temperature in the storage tank were also found as: 4375 kPa and 93 °C. Oil measurements have also been conducted to track oil slippage between the two stages with different target pressures and run times. Experimental testing has shown that the dominant factor affecting oil slippage in a two stage compressor system is pressure ratio. A simulation model has been developed to predict the compressor performance. The model predictions have been validated by using the test data.
- The simulation studies presented in this paper employed a simple element approach and lump system method to model the compressor dynamic process and pressurized tank. This leads to some inaccuracy, since it is difficult to predict the mass flow rate accurately using this approach. In addition, the temperature calculations are not as accurate as desired due to the existence of the intercooler and heat transfer between the compressor shells and the surrounding air. Future work should therefore include the usage of a more accurate differential model. Additionally, the heat transfer and back pressure calculations should be investigated, which will lead to a better understanding of the actual two stage compressor dynamic process.

## NOMENCLATURE

| | | |
|---|---|---|
| $\eta_v$ | volumetric efficiency | (–) |
| $n$ | speed of compressor | (r) |
| $m$ | expansion efficiency | (–) |
| $V_h$ | displacement | ($m^3$) |
| $\lambda_p$ | pressure coefficient | (–) |
| $\lambda_l$ | leakage coefficient | (–) |
| $\lambda_T$ | temperature coefficient | (–) |
| $\lambda_\phi$ | condensation coefficient | (–) |
| $C$ | clearance volume factor | (–) |
| $\rho$ | density | (kg/$m^3$) |
| $u$ | specific internal energy | ($kJ/kg$) |
| $t_{step}$ | time in each loop | (s) |
| $h$ | convection coefficient | ($kJ/m^2 - K$) |
| $A$ | heat transfer area | ($m^2$) |

**Subscripts**

| | |
|---|---|
| $d$ | discharge |
| $dis$ | discharge |
| $s$ | suction |
| $e$ | experimental |
| $th$ | theoretical |
| $L$ | entering tank |

## REFERENCES

Elhaj, M., Gu, F., Ball, A., Albarbar, A., Al-Qattan, M., and Naid, A. (2008). Numerical simulation and experimental study of a two-stage reciprocating compressor for condition monitoring. *Mechanical Systems and Signal Processing*, 22(2):374–389.

MacLaren, J. and Kerr, S. (1969). Paper 3: An analytical and experimental study of self-acting valves in a reciprocating air compressor. In *Proceedings of the Institution of Mechanical Engineers, Conference Proceedings*, volume 184, pages 24–33. SAGE Publications.

Ndiaye, D. and Bernier, M. (2010). Dynamic model of a hermetic reciprocating compressor in on–off cycling operation (abbreviation: Compressor dynamic model). *Applied Thermal Engineering*, 30(8):792–799.

## ACKNOWLEDGEMENT

The authors would like to thank BlackPak Inc. for sponsoring and providing the compressor box for testing.